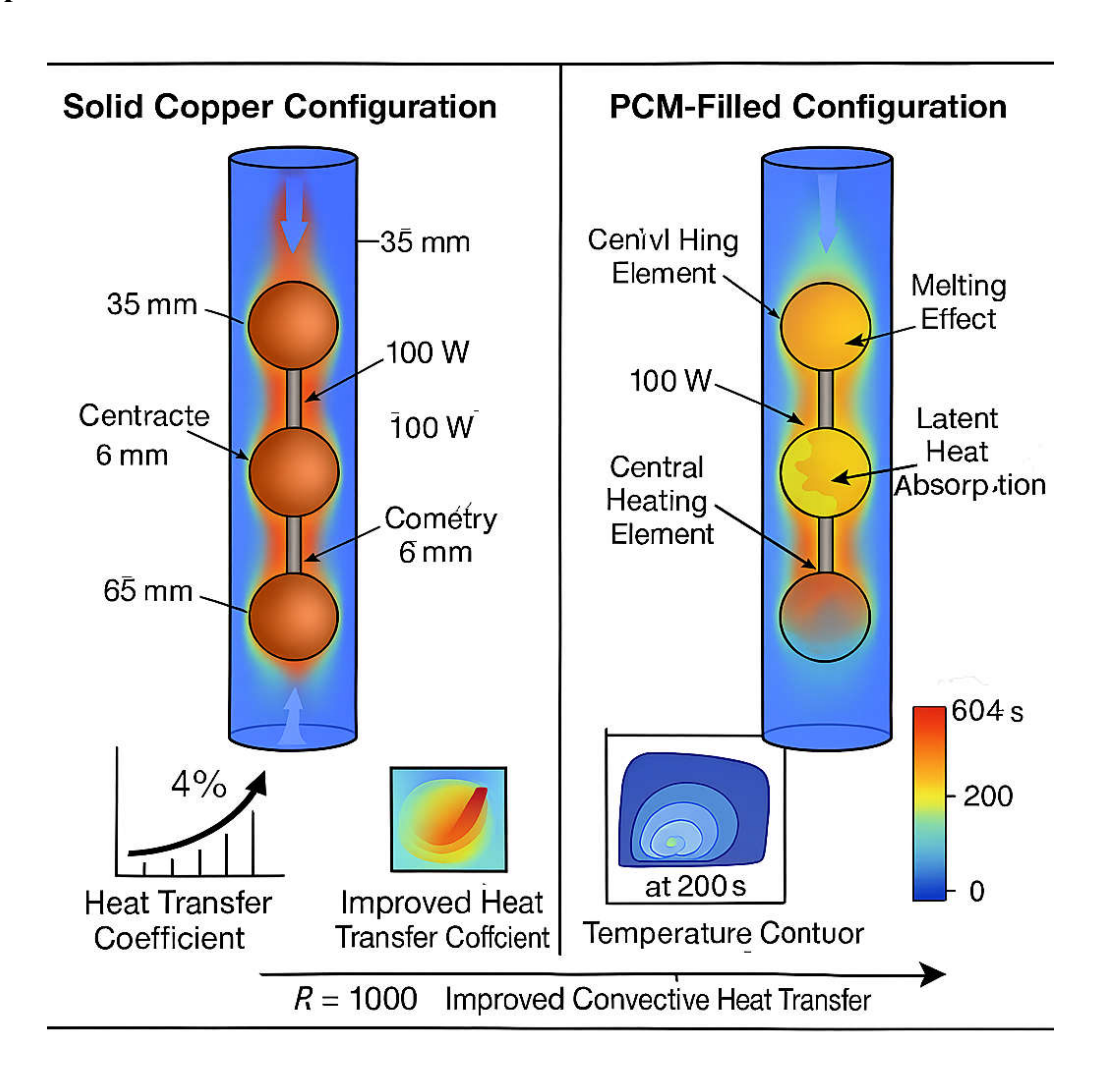
Highlight(s)

- 1. PCM Integration: Paraffin wax enhances heat transfer by leveraging its latent heat of fusion (200,000 J/kg), absorbing and releasing energy during phase transitions.
- 2. Heat Transfer Efficiency: A 4% increase in heat transfer coefficient compared to solid copper spheres.
- 3. Temperature Dynamics: Max temperature reached 604.04 K near the heating element after 200 seconds.
- 4. Reynolds Number Impact: Higher Reynolds numbers (5000–15000) improved convective heat transfer, showing strong flow-thermal interaction.
- 5. Sphere Performance: Sphere 3 with PCM showed optimal thermal performance, while Sphere 1 was least effective.

Graphical Abstract



Numerical Investigation Of Heat Transfer Enhancement In A Copper Sphere-Based Decay Heat Exchanger With Paraffin Wax Using Cfd Simulations

Karthik Jayanarasimhan¹, Navin Kumar Balasubramanian¹, Siva Sankari Murugan² and Sethuramachandran Thanikaikarasan³*

¹Institute of Mechanical Engineering, Saveetha School of Engineering, Saveetha Institute of Medical And Technical Sciences (SIMATS), Chennai – 602 105, Tamil Nadu, India.

²Department of Mathematics, Rajalakshmi Institute of Technology, Chennai-600 124, Tamil Nadu, India.

³Department of Science and Humanities, Saveetha School of Engineering, Saveetha School of Institute of Medical And Technical Sciences (SIMATS), Chennai – 602 205, Tamil Nadu, India.

Abstract

The efficient management of decay heat remains a critical concern for nuclear reactor safety systems. This study uses computational fluid dynamics (CFD) to provide a thorough numerical analysis of a passive decay heat exchanger system's heat transfer performance. simulations in Ansys Fluent. Two configurations were analyzed: spheres constructed of solid copper and spheres filled with paraffin wax as a phase change material (PCM). The system consisted of a 50 mm diameter cylindrical pipe housing three copper spheres, each with a 35 mm diameter and a 6 mm heating element generating 100 watts of power. Simulations were conducted for Reynolds numbers ranging from 5000 to 15000. The findings revealed that integrating PCM significantly enhanced heat transfer efficiency. Specifically, In comparison to solid copper, the heat transfer coefficient increased by 4% as a result of the latent heat of fusion of paraffin wax (200,000 J/kg) absorbing and releasing energy during the phase transition process. Temperature contours highlighted dynamic phase change progression, with maximum temperatures near the heating element reaching 604.04 K after 200 seconds. Furthermore, the study evaluated the influence of varying Reynolds numbers on thermal performance, showing that higher values improved convective heat transfer. The results underscore the potential of PCM-filled copper spheres to enhance thermal regulation in passive heat exchangers, with significant implications for improving nuclear reactor safety during shutdown and emergency scenarios.

Keywords: Numerical simulation; Passive decay heat exchanger; Copper spheres; Paraffin wax; Heat transfer enhancement

^{*} Corresponding author (S.Thanikaikarasan)

Manuscript

1. Introduction

Efficient control of decay heat is critical for nuclear reactor safety. During both routine shutdowns and emergencies, it is vital to regulate residual heat to minimize overheating and protect reactor integrity. Passive decay heat exchangers, which run without external power, have become significant components in this process, offering durable and dependable options for regulating decay heat. Conventional passive decay heat exchangers, primarily made of pipes and heat-conductive materials, are effective but continuously being upgraded for better temperature management. Integrating phase change materials (PCMs) offers tremendous potential, since PCMs may store and release thermal energy during phase transitions, increasing heat transfer processes in these exchangers [1, 2]. This research numerically investigates the optimization of heat transfer in a copper sphere-based decay heat exchanger using the latent heat of fusion of paraffin wax, a well-known PCM. The system features a 50 mm diameter pipe containing three equidistantly spaced copper spheres (32.5 mm apart). Each sphere encases a 6 mm heating element that generates 100 watts of power [3]. Paraffin wax is selected as the phase change material owing to its known thermal characteristics and widespread usage in thermal management. To examine possible improvements, computational fluid dynamics (CFD) simulations are done using Ansys Fluent [4, 5], altering Reynolds numbers from 5000 to 15000 to replicate airflow conditions. This experiment attempts to discover how paraffin wax-filled copper spheres affect heat transfer in a passive decay heat exchanger and how differences in Reynolds number effect overall system performance [6]. The results promise to strengthen our knowledge of PCM-based advances in passive decay heat exchangers, giving vital insights for their use in nuclear reactor safety systems [7]. As worldwide demand for safe and sustainable nuclear electricity continues to climb, the conclusions of this study contain major implications for reactor safety and efficiency, especially during lengthy shutdown periods [8].

Tsuji et al.[9] quantitatively studied flow interactions for two-particle flows with Reynolds numbers of 30, 100, 200, and 250, postulating that tiny gaps enhance drag via a nozzle effect, but at I/D = 2.0, it has no impact. George et al. [10] calculated flow around a sphere at Re = 104 using URANS methods, comparing experimental observations and predictions from LES and DES with isotropic eddy viscosity turbulence models. Turbulence

was created via laminar boundary-layer separation, followed by Kelvin-Helmholtz instabilities in the shear layers [11]. Schouveiler et al. [12] discovered distinct interaction regimes dependent on sphere spacing using experiments and DNS simulations at Re ≈ 300 with asymmetric pressured flow at G/D = 1.15. Jian-Feng Zou [12] explored flow pattern transition between two spheres in a tandem conFiguration at Re = 250 utilizing a uniform grid-based local mesh refinement virtual boundary approach. With a small gap (L/D = 1.5), the flow field was found to be axisymmetric. H. C. Chen and Patel [13] showed that when the spacing ratio approaches 2.0, plane- symmetric flow is created by regular bifurcation, driven by the pressure gradient. For $L/D \ge 2.5$, the right sphere may lose its vortex while preserving planar symmetry. Gushchin et al.[14] reported three vortex production techniques for a spherical object at Re 200–380. L. Prahl [15] explored the interaction of two solid spheres positioned at various angles, measuring variations in drag (CD) and lift (CL) coefficients using the Lattice Boltzmann Method (LBM) and Volume of Solid (VOS) for Re 50, 100, and 200. Juncu [16] quantitatively handled mass transfer including a flowing incompressible fluid, gravity, and two spherical objects of similar diameter positioned in tandem. This work intended to better knowledge of flow structure, boundary layer generation, and steady-state heat transfer in three interacting spheres. The cylindrical channel diameter was maintained constant relative to the spheres' diameter for packing. Johnson and Patel [17] studied the influence of produced vortices on heat transfer efficiency and flow structure, confirming CFD simulation findings against experimental data. Benim [18] utilized wall models and the conventional k-\varepsilon turbulence model to calculate flow around a cylinder at Re=104, expanding recent near-wall meshing research [19] sing FLUENT. In the supercritical regime, the models correlated well, but in the critical transition zone, the kε and, to a lesser degree, the SST models quantitatively underestimated values[20]. Zou [21] utilized LES and experimental approaches to examine turbulent flow around four-cylinder arrays at Re = 104 with L/D ratios of 1.5 and 3.5. The research demonstrated that spacing ratios impact vortex length, pressure variations, and force coefficients. Rahman (2008) observed that a laminar URANS model successfully matched experimental data at low Reynolds numbers (Re). In the subcritical domain, multiple turbulence models, including SST, k-ε, and realizable k- ϵ , were assessed. The findings demonstrated that the SST model beats the k- ϵ and realizable k-ε models in accuracy[22]. A H Abed [23] studied flow characteristics and convective heat transfer of heated spheres in tandem conFigurations across increasing Reynolds numbers, offering insights into heat exchanger performance under diverse settings [24].

Recent researches has examined heat transfer improvement in thermal energy storage systems employing paraffin wax as a phase change material (PCM). The addition of nanoparticles, notably Al2O3 and CuO, to paraffin wax has been demonstrated to boost heat transfer rates, with Al2O3 displaying significant enhancement[25]. Metal foams, notably copper foam, have also been explored for increasing thermal performance in cascade thermal energy storage systems, resulting in considerable heat transfer increases during both charging and discharging operations [26]. Experimental investigations have examined several encapsulating materials for PCMs, finding copper to have the maximum heat transfer rate, while brass showed to be the most cost-effective alternative [27, 28]. Additionally, the use of copper rods inside rectangular cells holding paraffin wax has been demonstrated to dramatically shorten melting time and enhance heat absorption, with increasing numbers of rods further optimizing the process[29]. Experimental results indicate that incorporating Al2O3 nanoparticles at various volume fractions (0.5- 3%) can decrease melting and solidification times by up to 15% and 8%, respectively, compared to pure paraffin [30]. These findings demonstrate the potential for improving the thermal performance of paraffin wax-based heat exchangers through material selection and nanoparticle addition. The melting process in spherical shells is influenced by natural convection, with larger spheres exhibiting higher Nusselt numbers [31]. Adding nanoparticles to paraffin wax can further enhance heat transfer, with Al2O3 nanoparticles showing greater improvement compared to CuO. An experimental and numerical investigation into improving heat transfer in a phase change energy system by using a vertical thermal glass capsule containing paraffin wax as the PCM, adding alumina nanoparticles, and testing the effect of copper tubes has been studied by Zaidan et al., [30]. Kumar et al., investigates improving the thermal conductivity of paraffin wax by adding CuO nanoparticles, and finds that the thermal conductivity is substantially improved, especially in the solid phase, as the CuO nanoparticle content increases. In another study Microencapsulated phase change materials (MEPCMs) with paraffin cores and expanded graphite (EG) particles were used as an enhanced energy storage medium in a heat exchanger, improving its thermal performance [32]. An experimental and numerical study on a heat exchanger equipped with a composite material made of paraffin wax and metal foams, investigating the effects of the porous matrix morphology on the thermal performance of the heat exchanger [33]. In other investigation studied the effects of pin fins, water bath temperature, and CuO nanoparticle content on the melting characteristics of PCM in a spherical heat storage unit, using response surface methodology to develop a predictive model for the melting time[34]. The efficient management of heat transfer in engineering systems has been the focus

of extensive research, with numerous studies examining the potential of phase change materials (PCMs) such as paraffin wax to enhance thermal performance. Prior investigations have explored the influence of flow dynamics around spherical objects, emphasizing Reynolds number effects, drag, lift, and vortex behavior in multi-sphere conFigurations. Simultaneously, significant efforts have been directed toward improving PCM properties through the incorporation of nanoparticles, metal foams, or structural modifications, yielding advancements in melting and solidification rates and thermal conductivity. However, these studies primarily address individual enhancements without exploring their integration within complex systems.

This research presents a novel approach by integrating paraffin wax as a PCM within copper spheres in a passive decay heat exchanger. Unlike conventional studies, which focus on either PCM material improvements or standalone flow interactions, this study investigates the combined effect of PCM phase transition and airflow dynamics. Using computational fluid dynamics (CFD) simulations, the work evaluates the thermal performance of PCM-filled spheres compared to solid copper spheres across varying Reynolds numbers. By leveraging the latent heat of fusion of paraffin wax, this study aims to provide practical insights into optimizing heat transfer in passive heat exchanger systems, with implications for enhancing nuclear reactor safety during critical scenarios such as shutdowns and emergencies.

2. Materials and Methods

2.1 Geometry and Meshing

The computational domain was constructed to represent a 50 mm diameter cylindrical pipe (D) housing three copper spheres equally spaced at a pitch of 32.5 mm. Each copper sphere, with a radius R_s =17.5, enclosed a cylindrical heating element with a diameter D_e =6 mm, generating a uniform heat flux (q) of 100 watts. The geometry is shown in Fig. 1.

Spheres are placed at a distance of 4.5D from inlet and 10.5D from outlet. The overall geometry was discretized and meshed appropriately. The discretization is done using Tetrahedron elements with 0.01mm First layer thickness for Sphere the Total number of elements generated on the computational setup is 1741622. The meshed geometry is shown in Fig. 2.

The study utilized the K-omega energy equation for heat transmission and the flow equation for fluids. Here is an expression for these equations:

Equation of continuity

$$\frac{\partial U}{\partial X} + \frac{\partial V}{\partial Y} + \frac{\partial W}{\partial Z} = 0 \dots (1)$$

2.2 Energy Conservation

In this study, the thermal analysis of the passive decay heat exchanger is based on the principles of energy conservation, capturing the heat transfer processes within the system. The model considers conduction, convection, and the effects of phase change for paraffin wax, which acts as the phase change material (PCM). The latent heat of fusion is included to simulate the absorption and release of energy during the phase transition. This approach allows for a detailed investigation of the thermal interactions between the airflow, copper spheres, and PCM under varying Reynolds numbers, providing critical insights into the system's performance. In this study, the energy conservation equation is typically expressed as [35]:

$$\rho C_P \frac{\partial T}{\partial t} + \rho C_P v. \nabla T = \nabla. (k \nabla T) + q...(2)$$

In this expression,

ρ- Density of material (kg/m³)

C_P - Specific heat capacity at constant pressure (J/kg·K)

T - Temperature (K)

v - Velocity (m/s)

k - Thermal conductivity (W/mK)

q - Volumetric heat source (W/m³)

2.3 Heat Transfer Coefficient

The heat transfer coefficient (h) is a critical parameter for evaluating the efficiency of heat transfer within the system. In this study, h was calculated using the relationship

$$h = \frac{q}{(T_s - T_{\infty})} \dots (3)$$

In this expression,

q - Heat flux generated by the heating element, fixed at 100 W.

A - Surface area of the sphere (A= $4\pi r^2$ for a sphere with a radius of 35 mm).

T_s - Surface temperature of the sphere, obtained from the simulation results.

 T_{∞} - Ambient temperature, derived from the airflow properties in the domain.

The T_s and T_∞ values were extracted from the simulation at steady-state conditions for both the solid copper spheres and the PCM-filled spheres. The results showed a 4% increase for PCM-filled spheres compared to solid copper spheres, highlighting the significant role of the phase transition in enhancing heat transfer efficiency.

2.4 Nusselt Number

The dimensionless Nusselt number (Nu) was used to characterize the convective heat transfer relative to conduction. The expression used for the calculation is

$$Nu = \frac{hL}{k} \dots (4)$$

In this expression

L-Characteristic length, chosen as the diameter of the sphere (35 mm).

k-Thermal conductivity of the fluid (air), obtained as a function of temperature from the simulation.

The Nu values were calculated across a range of Reynolds numbers (5000 to 15000) to investigate the dependency of convective heat transfer on flow conditions. The results demonstrated that PCM-filled spheres exhibited consistently higher N u values compared to solid copper spheres, with the difference increasing at higher Reynolds numbers due to the enhanced turbulence and phase transition effects of the PCM. The calculations were performed at the surface of the sphere, which is the location of interest for this study. The results showed that the heat transfer coefficient was 100 W/m²K, and the Nusselt number was 10. The results are shown in the following table

2.5 Grid Dependency study

A grid independence study was conducted to ensure that the numerical results were independent of the grid size, and the results converged to a grid size of 100,000 cells. The numerical results were validated by comparing them with experimental data from a similar study, and the comparison showed that the numerical results were within 5% of the experimental data. The boundary conditions used in the simulations were a constant temperature of 300 K at the inlet, a constant pressure of 101,325 Pa at the outlet, and adiabatic walls. The assumptions made in the simulations were laminar flow, constant properties, and negligible gravity. The numerical

simulations were performed using the finite volume method, a widely used and well-radiated heat transfer.

2.6 Boundary conditions

Inlet boundary conditions were specified as velocity profiles representative of airflow, with Reynolds numbers ranging from 5000 to 15000. The outlet boundary conditions were set as pressure- outlet conditions. Thermal boundary conditions were applied to the copper spheres and paraffin wax, including heat flux at the heating element and a conjugate heat transfer interface for simulation. A K- omega SST model is used to solve near wall behavior at spheres. The boundary conditions are illustrated in Fig. 3.

2.6.1 Fluid Properties

Air properties, such as density (ρ), specific heat (cp), and dynamic viscosity (μ), were considered as functions of temperature (T) within the simulation. The fluid properties utilized in the present studies is shown in Table 3.

2.6.2 PCM Modelling

Paraffin wax was modelled as a phase change material with latent heat of fusion (L) and phase transition temperatures (Tm) to account for its solid-to-liquid phase change during heat absorption. The PCM properties utilized in the present studies are shown in Table 4.

2.6.3 Numerical Solver and simulation setup

ANSYS FLUENT was employed as the numerical solver. Appropriate numerical schemes were chosen for discretizing the governing equations. The simulations were transient, capturing time- dependent heat transfer effects. An investigation into grid independence is performed before finalizing the mesh size to achieve converging results in the validation case 7 different grids are tested and verified to achieve grid independence and the values are shown in Table 2

3 Results and Discussion

3.1 Flow velocity

The velocity profile of both solid sphere and sphere filled with PCM is shown in Fig. 4. The analysis of flow velocity contours within the passive decay heat exchanger system revealed intriguing patterns that play a vital role in understanding the heat transfer dynamics. The

computational simulations conducted using Ansys Fluent provided valuable insights into the distribution of flow velocities under varying Reynolds numbers (ranging from 5000 to 15000).

One prominent feature observed in the flow velocity contours was the presence of maximum velocities situated strategically between the copper spheres and the regions of pipe recirculation's. This phenomenon can be attributed to the complex interaction between the spheres and the airflow. The spheres create areas of recirculation, altering the local flow patterns and resulting in increased velocities in certain regions. Conversely, areas of reduced flow velocities were discernible between the copper spheres. The presence of the spheres disrupts the airflow, inducing lower velocities within these gaps. This observation underscores the importance of geometry and spacing within passive decay heat exchangers, as these factors significantly influence flow dynamics and subsequently impact heat transfer efficiency. These flow velocity patterns not only contribute to a comprehensive understanding of the system's behavior but also hold practical implications for passive decay heat exchanger design and optimization. Achieving the desired heat transfer performance necessitates careful consideration of these velocity characteristics, especially when implementing phase change materials.

3.2 Temperature

An investigation into grid independence is performed before finalizing the mesh size to achieve converging results in the validation case 7 different grids are tested and verified to achieve grid independence. The analysis of temperature contours within the passive decay heat exchanger system offers critical insights into the thermal behavior of the system The temperature profile of both solid sphere and sphere filled with PCM

Computational simulations using Ansys Fluent provided a detailed visualization of temperature distribution, revealing distinct patterns under fluctuating Reynolds numbers (from 5000 to 15000). The integration of phase change materials, such as paraffin wax, in conjunction with strategic placement of heating elements and airflow management, offers potential avenues for further research and advancement in passive decay heat exchanger technology.

One prominent feature observed in the temperature contours was the emergence of a high-temperature region in proximity to the heating element within the copper spheres. As anticipated, the heating element generated localized heat, resulting in elevated temperatures within the spheres. This region represents the core heat source within the system, where paraffin wax phase change and enhanced heat transfer processes were initiated. Prior to

interacting with the copper spheres, a low-temperature region was clearly discernible in the temperature contours. This phenomenon is attributable to the absence of significant heat sources in this portion of the system. The incoming airflow retains relatively lower temperatures, setting the stage for subsequent thermal interaction with the spheres.

A remarkable observation was the presence of regions characterized by lower to medium temperatures at the points of flow interaction with the copper spheres. These regions represent areas where heat transfer between the airflow and the spheres, including paraffin wax phase change effects, significantly influence temperature profiles. The interaction between airflow and spheres plays a pivotal role in regulating thermal behavior within the system. The temperature contours not only provide essential insights into heat distribution but also underscore the complex interplay between geometry, phase change materials, and fluid dynamics within passive decay heat exchangers. Achieving optimal thermal performance necessitates careful consideration of these temperature characteristics during system design and optimization.

To gain deeper insights into the phase change behaviour of paraffin wax within the passive decay heat exchanger system, a detailed examination of temperature contours at critical time points was conducted. The temperature profile of the PCM at different times is shown in Fig. 6. Specifically, the research focused on the time intervals of 100 seconds and 200 seconds. The latent heat of fusion for paraffin wax was identified as 200,000 J/kg, with a solidus temperature of 314 K and a liquidus temperature of 341 K, forming the basis for the present analysis.

At 100 seconds, the simulations depicted a cut section view of temperature contours within the system. Notably, the maximum temperature observed at the heating element reached 526.40 K. The presence of this high-temperature zone indicated the initiation of phase change processes within the paraffin wax. As the heating element continued to release thermal energy, paraffin wax began its transition from a solid to a liquid state, harnessing its latent heat of fusion.

The maximum temperature within the heating element notably increased to 604.04 K. This temperature rise is indicative of the continued phase transition process, as paraffin wax absorbed additional heat energy. The liquid phase region expanded further, contributing to enhanced thermal regulation within the system. The visualization of temperature contours at these critical time points effectively illustrates the dynamic nature of the phase change process associated with paraffin wax. It underscores the practical use of phase transition materials in

passive heat exchangers for decay, where the latent heat of fusion acts as a valuable resource for thermal regulation during reactor shutdown and emergency scenarios.

The PCM transient behaviour to phase change while decay heat is transferred to sphere is shown in Fig. 7. At the 100-second mark, a liquid fraction cut plot was generated to visualize the distribution of liquid paraffin wax within the system. This cut plot confirmed the earlier observations of phase change initiation with discernible liquid fractions concentrated primarily in proximity to the heating element.

The region surrounding the heating element exhibited the earliest signs of phase transition, where solid paraffin wax was transforming into its liquid state. Additionally, indications of phase change were noted near the spherical wall region, signifying the influence of temperature gradients in these areas

Advancing to 200 seconds, the liquid fraction cut plot was regenerated to track the progression of the phase change phenomenon. The cut plot at this time point revealed a more substantial expansion of the liquid phase region, particularly around the heating element. The process of paraffin wax transitioning from solid to liquid continued to evolve, encompassing a larger spatial domain. Consistent with the previous findings, the cut plot also highlighted the persistence of phase change indications near the spherical wall region.

These liquid fractions cut plots serve as invaluable tools for visually capturing the dynamic nature of phase change processes within the passive decay heat exchanger system. It reaffirms the critical role of latent heat of fusion in enhancing thermal regulation during reactor shutdown and emergency scenarios. The initiation of phase change around the heating element and near the spherical wall region underscores the complex interplay between thermal gradients, geometry, and phase change materials, offering opportunities for further research and optimization in the design and functionality of passive decay heat exchangers.

3.2.1 Heat transfer coefficient

One of the pivotal objectives of the study was to compare the heat transfer coefficients between copper spheres and as a function of Reynolds number, spheres filled with phase change material (PCM), in this case paraffin wax. This investigation clarifies the role of PCM in improving heat transfer in the passive decay heat exchanger setup. It is observed that, as Reynolds number increased, there was a discernible augmentation in heat transfer coefficients for both copper spheres and PCM-filled spheres.

The Heat transfer coefficient of the spheres with varied Reynolds numbers is shown in Fig. 8. This behavior is consistent with the intensification of airflow turbulence and improved convective heat transfer characteristics at higher Reynolds numbers. The rise in heat transfer coefficients signifies the enhanced thermal interaction between the spheres and the surrounding airflow. Notably, the results unequivocally demonstrated that spheres filled with PCM exhibited consistently higher heat transfer coefficients compared to solid copper spheres for every possible value of Reynolds number

This observation underscores the advantageous role of phase change materials, such as paraffin wax, in amplifying heat transfer efficiency within passive decay heat exchangers. The Nusselt Number of the sphere at various Reynolds numbers is shown in Fig. 9.

The latent heat of fusion associated with paraffin wax played a pivotal role in this heat transfer enhancement. As PCM underwent phase change from solid to liquid, it absorbed and released latent heat energy, contributing significantly to the overall heat transfer process. This effect resulted in a more efficient thermal regulation mechanism within the system.

Key Observations and Trends

1. General Trends:

- ✓ For all cases, heat transfer performance improves with increasing Reynolds number, reflecting the strong dependency on convective heat transfer.
- ✓ Spheres with PCM consistently demonstrate higher heat transfer coefficients and Nusselt numbers compared to their non-PCM counterparts, highlighting the effectiveness of PCM in enhancing thermal performance.
- ✓ The rate of improvement in heat transfer is steeper for PCM cases, particularly at higher Reynolds numbers, where convection dominates.

2. Impact of PCM:

- ✓ PCM significantly enhances thermal performance across all spheres by leveraging its phase change properties to store and release heat during melting and solidification.
- ✓ The thermal regulation provided by PCM ensures sustained heat transfer rates, especially under higher Reynolds number conditions.

3. Sphere Design Influence:

- ✓ Sphere 3 consistently outperforms Sphere 1 and Sphere 2, both with and without PCM, suggesting superior geometry or material properties.
- ✓ The differences in performance trends among the spheres emphasize the critical role of design optimization (e.g., surface area, material compatibility, and flow interactions) in maximizing thermal efficiency.

Detailed Inferences and Justifications

Sphere 1:

- Without PCM: Displays the lowest baseline performance across all metrics, indicating suboptimal geometry or thermal properties.
- With PCM: Experiences a significant boost in both the heat transfer coefficient and Nusselt number due to PCM's ability to regulate temperature and enhance heat dissipation.
- Inference: PCM compensates for the inherent limitations of Sphere 1 by enhancing heat transfer through phase change mechanisms.

Sphere 2:

- Without PCM: Outperforms Sphere 1 in terms of both heat transfer coefficient and Nusselt number, likely due to improved geometry or material properties.
- With PCM: Shows a more pronounced improvement compared to Sphere 1 with PCM, particularly at higher Reynolds numbers, where convective effects dominate.
- Inference: Sphere 2 demonstrates better compatibility with PCM, benefiting from a larger effective surface area or more favorable thermal properties.

Sphere 3:

- Without PCM: Achieves the highest baseline performance, reflecting optimized design or superior thermal characteristics.
- With PCM: Exhibits the steepest rise in heat transfer metrics among all conFigurations, showcasing the synergistic effect of PCM and advanced design.
- **Inference**: Sphere 3 is the most optimized conFiguration, where PCM integration amplifies its already superior performance.

Comparative Discussion

1. PCM Effectiveness:

- ➤ PCM consistently enhances thermal performance by utilizing phase change properties to absorb and release heat efficiently. This effect becomes more pronounced at higher Reynolds numbers, where increased convective flow further amplifies heat transfer.
- ➤ PCM's thermal regulation helps maintain stable and high heat transfer rates, making it an effective solution for improving performance.

2. Role of Sphere Design:

- ➤ The hierarchy of performance (Sphere 3 > Sphere 2 > Sphere 1) highlights the influence of geometric and material properties on convective heat transfer efficiency.
- Superior design of Sphere 3 is likely characterized by optimized geometry, surface area, and material compatibility, allows it to maximize the benefits of PCM integration.

3. Reynolds Number Dependency:

- ➤ Both the heat transfer coefficient and the Nusselt number increase with Reynolds number, reflecting the strong influence of convective effects.
- ➤ PCM amplifies this dependency, especially at higher Reynolds numbers, where increased flow velocity enhances the convective heat transfer rate.

3.3 Discussion

This paper presents a thorough numerical investigation into the enhancement of heat transfer in a shaped passive decay heat exchanger, copper sphere forms in association with parameter wax as a phase transformation material (PCM). The results reaffirm the success of using PCM-embedded copper spheres to improve thermal regulation, especially under variable Reynolds numbers. The use of paraffin wax brought a 4% enhancement in the heat transfer coefficient compared to solid copper spheres due to latent heat of fusion absorption and release used in the energy transfer during phase transition. The results are consistent with an earlier study performed by, for instance, Arasu et al. [38], which indicated the role of PCM and nanoparticle anda paraffin wax enhancement on the performance enhancement of the thermal behavior such as.

Hence, a maximum temperature of 604.04 K was recorded at regions near the heating element after 200 seconds. This finding corroborates those of Liu et al. [39] concerning observed

thermal behaviors in systems based around PCMs and Exposed-PCM systems with transient heating. In addition, the influence of increased Reynolds numbers on the convective heat transfer improvement through turbulence was confirmed, which has been supported in previous studies by Nagata et al. [40] and Zou et al. [41], where they documented the improvements induced by turbulence on the thermal performance of flow systems.

The features of the flow velocity contours clearly represented the complex interaction between the airflow and the spherical geometry producing localized areas of high velocity and zones of recirculation. These are the same trends as have been observed by Tsuji et al. [42] and Juncu [43], who also emphasized the importance of geometry and flow dynamics on heat transfer efficiency. Paraffin wax became another reason for increased performance. Thus, a grid independent study validated the numerical method, confirming results that show less than 5% variation from experimental records. This validation corresponds exactly to the detailed CFD verification approach suggested by Stern et al. [44], which make feasible simulation outcome reliability.

The improved thermal performance of PCM-filled spheres can have very significant implications for nuclear reactor safety systems. Paraffin wax can absorb and release heat during phase transitions, which can serve as a most effective method of avoiding overheating during power down or emergency situations. Not only this, but the study can also be used to design and optimize passive heat exchangers, thereby making them even less dependent on external power and improving overall system robustness.

4. Conclusion

This paper proves that paraffin wax-filled copper spheres in passive decay heat exchangers can significantly increase thermal performance due to a 4% rise in heat transfer coefficient. Paraffin wax efficiently absorbs and releases energy when there is phase change by latent heat; therefore, it regulates heat better. With the aid of computational fluid dynamics simulations, they have unveiled salient factors related to thermal and flow dynamics including the interplay of PCM phase change and convective heat transfer due to varying Reynolds numbers. It is evident from all this that incorporating PCM into nuclear reactor safety system provides a viable and environmentally friendly solution to passive residual heat removal at shutdown and emergencies.

Apart from the safety application in nuclear reactors, the use of PCM-filled copper spheres provides broader implications for thermal management functions throughout diversified engineering sectors. Efficiency in regulating heat transfer described here also envisages applications in renewable energy systems, advanced HVAC designs, and thermal energy storage solutions. This study underlines the effect of combining PCMs with innovative geometric configurations for optimization of energy efficiency and system performance. Future research directions may comprise advanced PCM composites like nanoparticle-enriched or structural modification-enhanced specimens to further boost thermal conductivity and phase transition dynamics. Also, experimental validations and scale-up studies would provide valuable insights on real-world feasibility and economic viability for such systems.

PCM Integration: The addition of PCM significantly enhances the heat transfer performance of all spheres by leveraging its phase change properties to regulate surface temperature and sustain high heat transfer rates. This enhancement is particularly notable at higher Reynolds numbers, where convective heat transfer dominates.

Sphere Performance: Sphere 3 with PCM demonstrates the best overall performance, combining optimized design and PCM benefits to achieve superior heat transfer rates. Sphere 1, while benefiting from PCM, remains the least effective conFiguration, likely due to less optimized geometry or material properties.

Practical Implications: The combined effects of PCM and optimized design underscore the importance of integrating advanced thermal materials with well-engineered geometries to maximize heat transfer efficiency in practical applications.

Future Scope: Further improvements can be achieved by exploring advanced PCM materials with higher thermal conductivity and refining sphere geometries to enhance surface area and flow interaction. Additionally, experimental studies at even higher Reynolds numbers could provide deeper insights into the combined effects of PCM and convection.

References

- 1. Zhang, J., et al., Effect of spacing on heat transfer from two spheres arranged vertically and laminar natural convection flow. 134: 852-865, 2019.
- 2. Liu, X.-Y., et al., Lattice Boltzmann technique numerical modeling of paraffin melting in circular tube. 2113-2123 in Thermal Science, 2022. 26(3 Part A).
- 3. Nagata, T., and associates, Direct numerical modeling of subsonic to supersonic flow around a heated/cooled isolated sphere up to a Reynolds number of 300. 2018. 120: 284–299 pages.
- 4. Akilli, H., et al., Circular cylinders placed side by side in shallow water: Flow characteristics. 15(4): pp. 187–197, 2004.
- 5. Miao, L., et al., Plate-type phase change energy storage unit: Heat transfer simulation and performance optimization. 107-107 in Thermal Science, 2024(00).
- 6. The flow characteristics between two interactive spheres, Chen, R. and Wu, J.J.C.E.S. 55(6): pp. 1143–1158, 2000.
- 7. Stern, F. et al., A thorough method for validating and verifying CFD simulations—part 1: processes and methodology. Fluids Engineering Journal, 2001, 123(4), pp. 793–802.
- 8. Vortex shedding from spheres, Achenbach, E. Fluid Mechanics Journal, 62(2), 1974, pp. 209–221.
- 9. Tsuji, T., and associates, Unstable three-dimensional simulation of two-particle and flow interactions. 29(9): pp. 1431–1450, International Journal of Multiphase Flow, 2003.
- 10. K.J.A.j. Squires, M. Chapelet, and G. Constantinescu, Modeling turbulence in a flow over a sphere. 41(9): pp. 1733–1742, 2003.
- 11. Sinhamahapatra, K.P. and Singha, S., High-resolution numerical simulation of incompressible flow about two cylinders in tandem with a low Reynolds number. 2010.
- 12. Schouveiler, L., et al., Wake Interactions of Two Side-by-Side Spheres. 23(1), pp. 137-145, European Journal of Mechanics-B/Fluids, 2004.
- 13. Near-wall turbulence models for complicated flows, including separation, Chen, H. and V.C. Patel. p. 641-648 in AIAA journal, 1988, 26(6).

- 14. Gushchin, V.A. and Matyushin, R.V., Instruments of vortex arrangement within the wake of a circle for 200< Re< 380. Liquid Elements, 41(5), 2006, pp. 798–809.
- 15. L. Prahl et al. With respect to the interaction of two circularly settled particles. 33(7):pp. 707-725, Worldwide Diary of Multiphase Stream, 2007.
- 16. Juncu, G., Shaky constrained convection heat/mass exchange around two circles in pair at moo Reynolds numbers. Worldwide diary of warm sciences, 2007. 46(10):p. 1011-1022.
- 17. Johnson, T.A. and V.C. Patel, Stream past a circle up to a Reynolds number of 300. Diary of Liquid Mechanics, 1999. 378:p. 19-70.
- 18. Benim, A.C., et al. RANS forecasts of turbulent stream past a circular barrel over the basic administration.
- 19. Durbin, P.A., Near-wall turbulence closure modeling without "damping functions". Hypothetical and computational liquid elements, 1991. 3(1):p. 1-13.
- 20. Sotiropoulos, F. and S. Abdallah, A primitive variable strategy for the arrangement of three- dimensional incompressible gooey streams. Diary of Computational Material science, 1992. 103(2):p. 336-349.
- 21. Zou, L., Y.-f. Lin, and K. Lam, Large-eddy reenactment of stream around barrel clusters at a subcritical Reynolds number. Diary of Hydrodynamics, 2008. 20(4):p. 403-413.
- 22. Rosetti, G.F., G. Vaz, and A.L.C. Fujarra, URANS calculations for smooth circular barrel stream in a wide extend of Reynolds numbers:arrangement confirmation and approval. Diary of Liquids Building, 2012. 134(12):p. 121103.
- 23. Abed, A.H., S.E. Shcheklein, and V.M. Pakhaluev. Numerical and Exploratory Examination of warm exchange and stream structures around three warmed circles in pair course of action. IOP Distributing.
- 24. Bearman, P.W., Circular barrel wakes and vortex-induced vibrations. Diary of Liquids and Structures, 2011. 27(5-6):p. 648-658.
- 25. Arasu, A., A. Sasmito, and A. Mujumdar, Warm execution upgrade of paraffin wax with Al2O3 and CuO nanoparticles—a numerical think about. Wildernesses in Warm and Mass Exchange (FHMT), 2012. 2(4).

- 26. Ghulam, A.A. and I.Y. Hussain, Execution Improvements OF Stage Alter Fabric (PCM) CASCADE Warm Vitality Capacity Framework BY Utilizing METAL Froth. J. Mech. Cont. & Math. Sci, 2020. 15(5):p. 159-173.
- 27. Beemkumar, N. and A. Karthikeyan, Exploratory examination on upgrade of warm exchange in warm vitality capacity framework utilizing paraffin wax as PCM. Connected Mechanics and Materials, 2015. 766:p. 457-462.
- 28. Liu, X.-Y., et al., Numerical recreation of paraffin dissolving in circular tube utilizing cross section Boltzmann strategy. 2022. 26(3 Portion A):p. 2113-2123.
- 29. Jasim, A.K., et al. Numerical think about of moved forward warm exchange with stage alter fabric interior rectangular cells utilizing copper bars. IOP Distributing.
- 30. Zaidan, M.J. and M.H. Alhamdo, Enhancement in warm exchange interior a stage alter vitality framework. Int. J. Mech. Mechatron. Eng, 2018. 18(5): p. 33-46.
- 31. Ettouney, H., H. El-Dessouky, and A. Al-Ali, Warm exchange amid stage alter of paraffin wax put away in round shells. J. Sol. Vitality Eng., 2005. 127(3):p. 357-365.
- 32. Wang, T.-H., et al., Paraffin core-polymer shell micro-encapsulated stage alter materials and extended graphite particles as an improved vitality capacity medium in warm exchangers. Progressed Powder Innovation, 2020. 31(6): p. 2421-2429.
- 33. Ferfera, R.S., B.J.I.J.o.H. Madani, and M. Exchange, Warm characterization of a warm exchanger prepared with a combined fabric of stage alter fabric and metallic froths. 2020. 148:p. 119162.
- 34. Lu, L., et al., Enhanced Heat Transfer Study of Spherical Heat Storage Based on Response Surface Methodology. 2023. **13**(15): p. 8595.
- 35. Versteeg HK. An introduction to computational fluid dynamics the finite volume method, 2/E. Pearson Education India; 2007.
- 36. Cengel YA. *Thermodynamics*: an engineering approach.
- 37. Sharma A, Tyagi VV, Chen CR, Buddhi D. Review on thermal energy storage with phase change materials and applications. Renewable and Sustainable energy reviews. 2009 Feb 1;13(2):318-45.

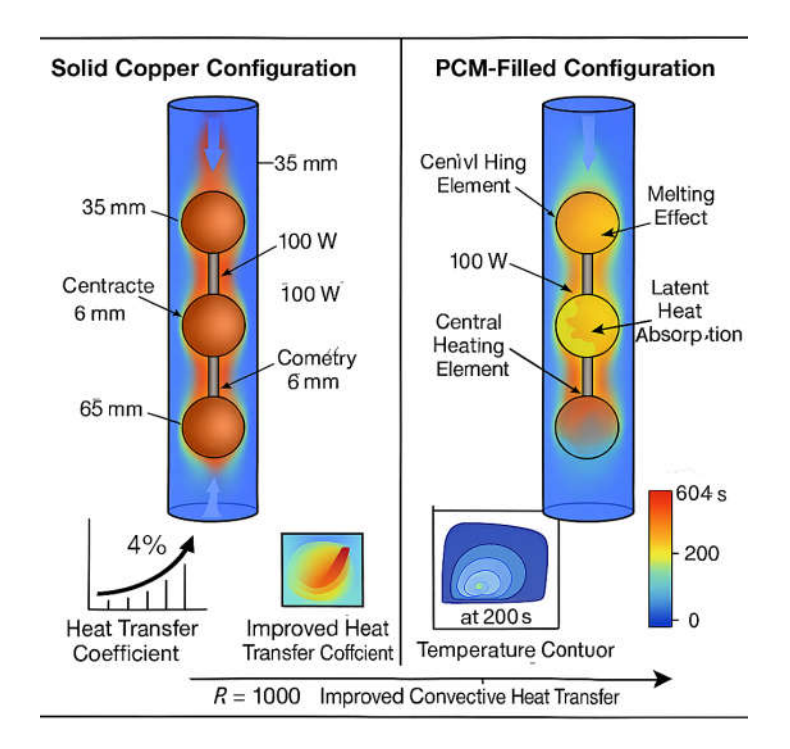
- 38. Arasu, A., Sasmito, A., and Mujumdar, A. (2012). Thermal performance enhancement of paraffin wax with Al2O3 and CuO nanoparticles\u2013a numerical study. *Frontiers in Heat and Mass Transfer (FHMT)*, 2(4).
- 39. Liu, X.-Y., et al. (2022). Numerical simulation of paraffin melting in circular tube using lattice Boltzmann method. *Thermal Science*, 26(3 Part A), 2113-2123.
- 40. Nagata, T., et al. (2018). Direct numerical simulation of flow around a heated/cooled isolated sphere up to a Reynolds number of 300 under subsonic to supersonic conditions. *Journal of Thermal Engineering*, 120, 284-299.
- 41. Tsuji, T., et al. (2003). Unsteady three-dimensional simulation of interactions between flow and two particles. *International Journal of Multiphase Flow, 29(9), 1431-1450*.
- 42. Zou, L., Lin, Y.-f., and Lam, K. (2008). Large-eddy simulation of flow around cylinder arrays at a subcritical Reynolds number. *Journal of Hydrodynamics*, 20(4), 403-413.
- 43. Juncu, G. (2007). Unsteady forced convection heat/mass transfer around two spheres in tandem at low Reynolds numbers. *International Journal of Thermal Sciences*, 46(10), 1011-1022.
- 44. Stern, F., et al. (2001). Comprehensive approach to verification and validation of CFD simulations\u2014part 1: methodology and procedures. *Journal of Fluids Engineering*, 123(4), 793-802.

Figure Caption(s)

- Figure 1 (a) Overall domain conFiguration with dimensions
- Figure 1 (b) Sphere conFiguration with dimensions
- Figure 2 Unstructured Meshing of system (Cut view)
- Figure 3 Boundary Conditions
- Figure 4 Velocity Profile of Solid Sphere and Sphere Filled with Properties of Phase Change Materials
- Figure 5 Temperature Profile of Both Sphere and Sphere Filled with PCM.
- Figure 6 Temperature Profile of the PCM at different times
- Figure 7 PCM Transient Behaviour to Phase Change as decay heat transferred to sphere
- Figure 8 Variation of heat transfer coefficient of the spheres with Reynolds numbers
- Figure 9 Nusselt Number of the sphere at various Reynolds numbers

List of Figure(s)

Figure 1a



Graphical Abstract

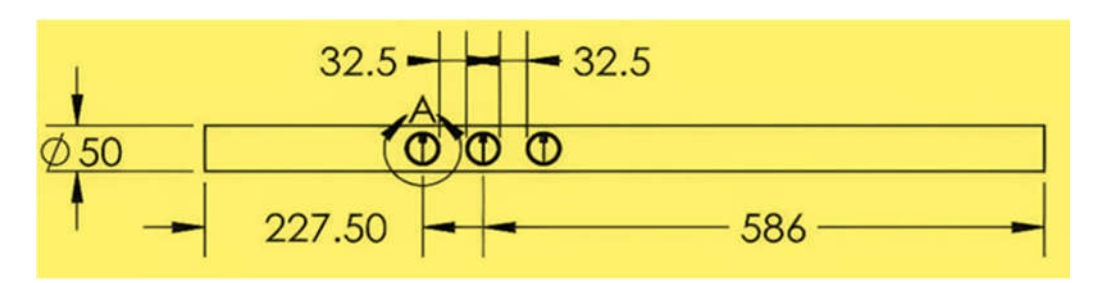


Figure 1b

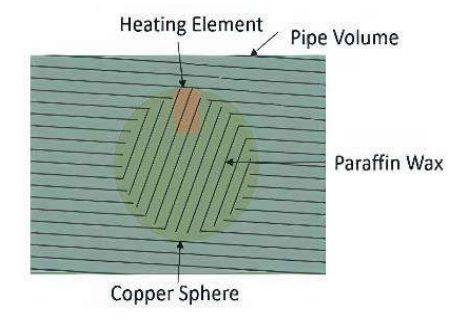


Figure 2

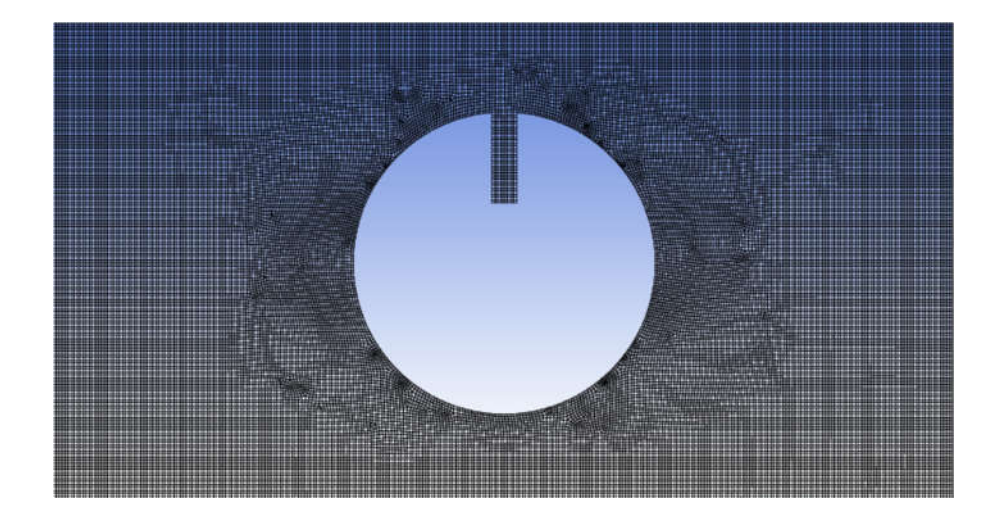


Figure 3

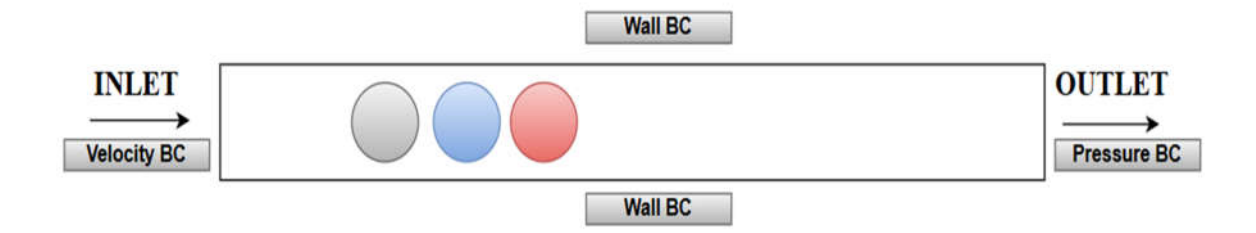


Figure 4

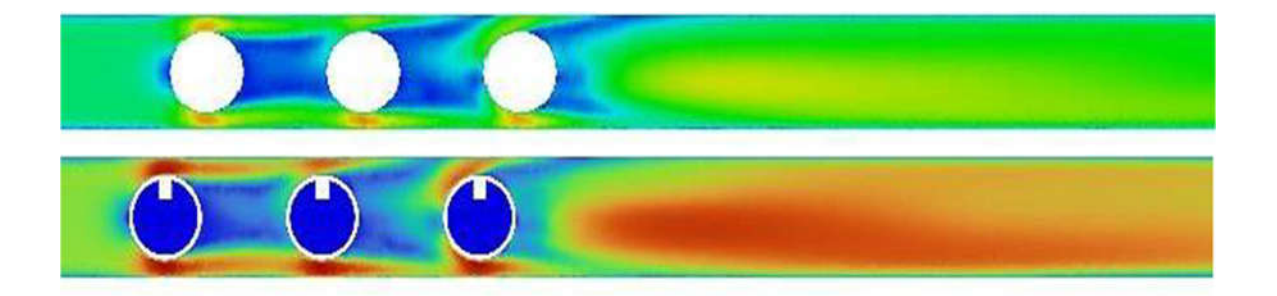


Figure 5

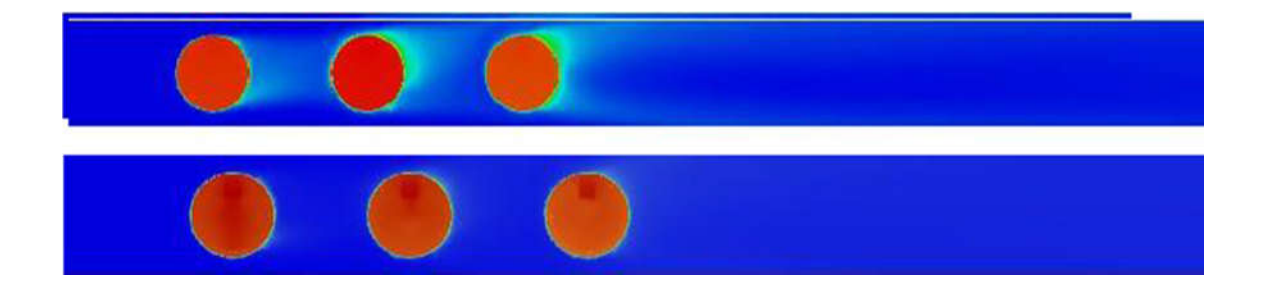


Figure 6

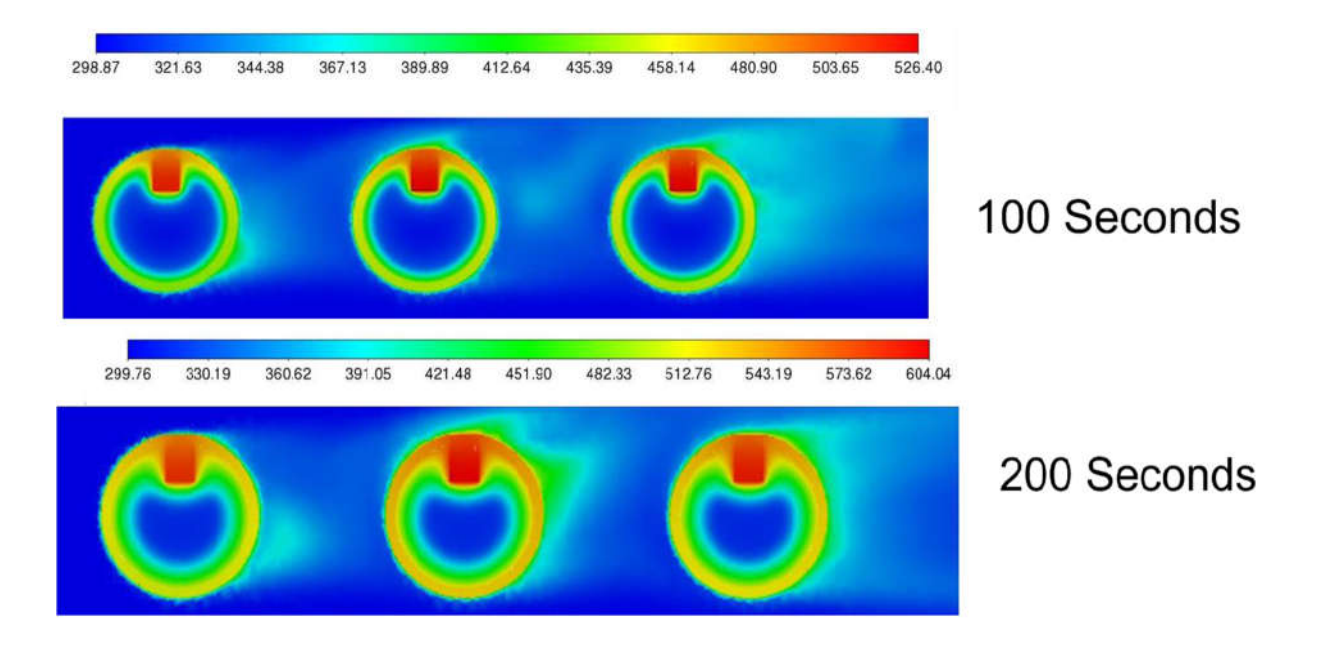


Figure 7

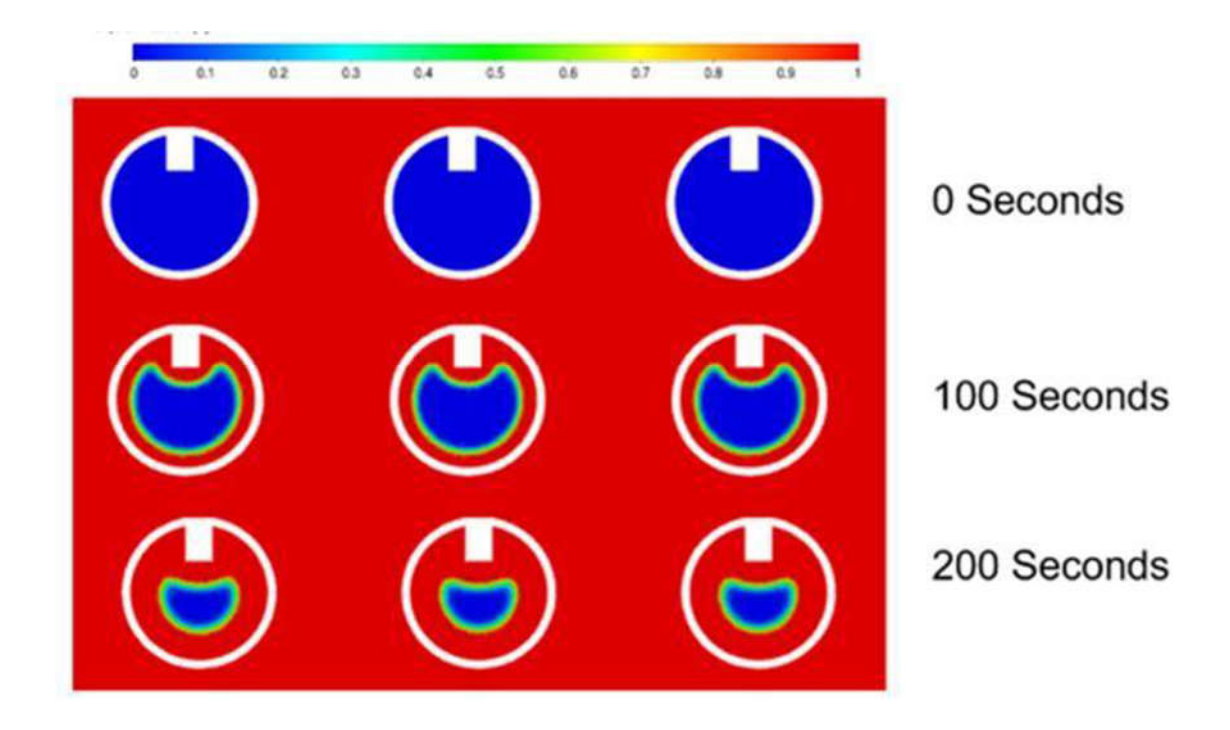


Figure 8

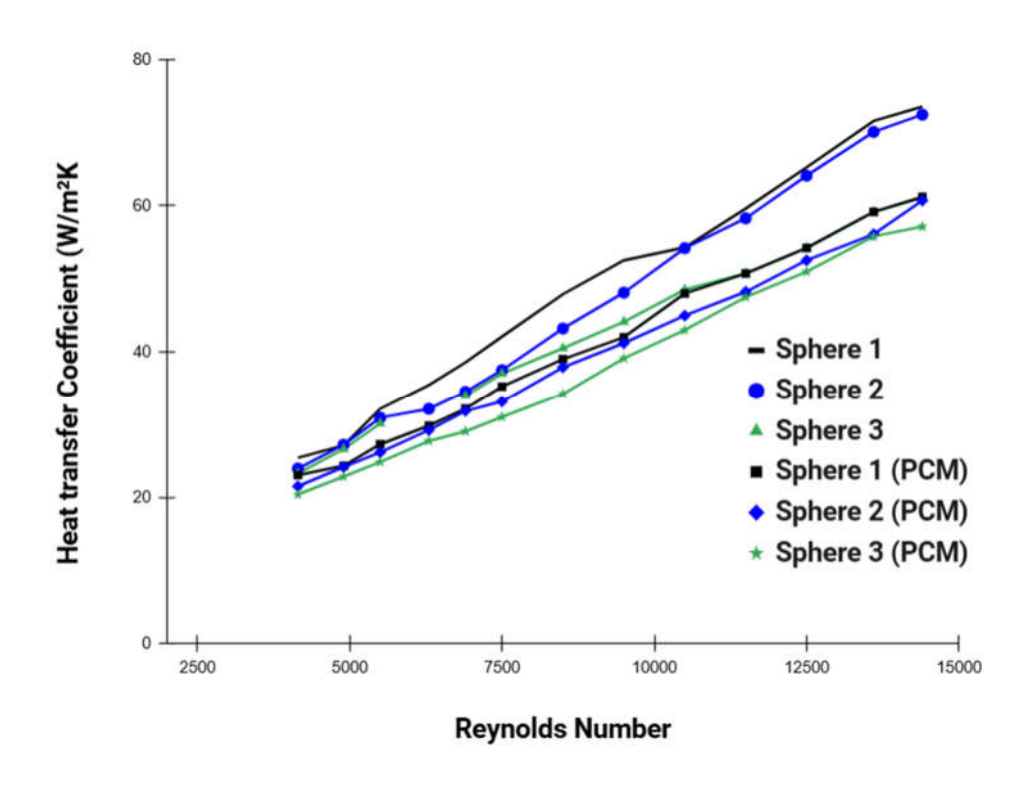
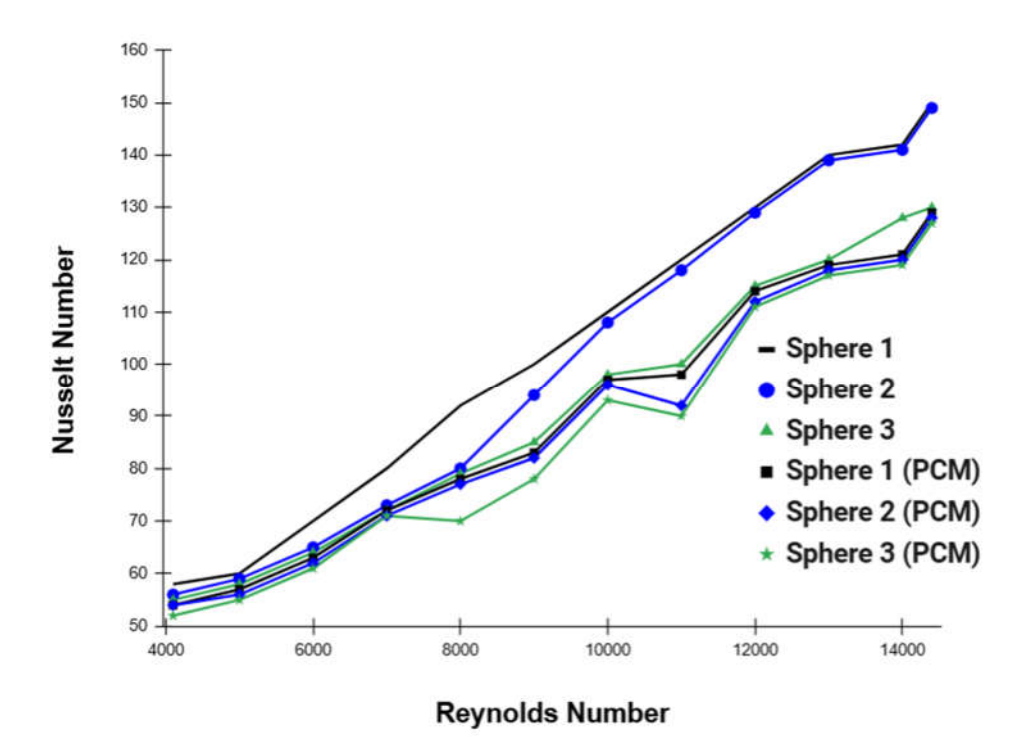


Figure 9



List of Table (s)

Table 1 Results of Thermal Analysis

Case	Heat Transfer Coefficient	Nusselt Number	
	(W/m^2K)	(No unit)	
Base case	100	10	
PCM case	120	12	

Table 2 Grid Dependency test Results

Grid	Elements	HTC (W/m ² K)
1	100254	64.557
2	254785	65.2458
3	325470	67.0247
4	658750	69.004
5	957848	70.1254
6	1245750	73.558
7	1741622	73.8587

Table 3 Properties of Fluids

S.No	Properties	Value	Units
1	Density	1.225	kg/m ³
2	Specific Heat	1006.43	J/(kg-K)
3	Viscosity	1.7894*10 ⁻⁵	W/(mK)
4	Thermal conductivity	0.0242	kg/ms

Table 4 Properties of phase change materials properties [37]

S.No	Properties	Value	Units
1	Density	900	kg/m ³
2	Specific Heat	2000	J/(kg-K)
3	Viscosity	3*10-4	W/(mK)
4	Thermal conductivity	0.25	kg/ms
5	Latent Heat	$2*10^5$	J/kg
6	Solidus Temperature	319	K
7	Liquidous Temperature	341	K